Comparative Biochemistry and Physiology, Part B 227 (2019) 21–30

Contents lists available at ScienceDirect

Comparative Biochemistry and Physiology, Part B

journal homepage: www.elsevier.com/locate/cbpb

Developmental dynamics of myogenesis in Pacific oyster *Crassostrea gigas*

Huijuan Li[a], Qi Li[a,b,*], Hong Yu[a,b], Shaojun Du[c]

[a] Key Laboratory of Mariculture (Ocean University of China), Ministry of Education, Qingdao 266003, China
[b] Laboratory for Marine Fisheries Science and Food Production Processes, Qingdao National Laboratory for Marine Science and Technology, China
[c] Institute of Marine and Environmental Technology, Department of Biochemistry and Molecular Biology, University of Maryland School of Medicine, Baltimore, MD, United States

ARTICLE INFO

Keywords:
Crassostrea gigas
Larvae
Myogenesis
Bivalves
Metamorphosis

ABSTRACT

Pacific oyster (*Crassostrea gigas*) is a sessile bivalve living in the intertidal zone. It has become an attractive model for developmental studies due to its metamorphic transition from a mobile planktonic larvae to a sessile adults. To determine the effect of metamorphosis on muscle development in oyster larvae, we characterized myogenesis during larval development and metamorphosis by phalloidin staining which labels filamentous actin filaments. Our data revealed a dynamic pattern of myogenesis during embryonic and larval development. It appears that simple "U-shaped" muscle ring first developed at the trochophore stage. This was followed by a more complex musculature including an anterior adductor, velum ventral retractors at the veliger stage, and the addition of posterior adductors and foot retractors at the veliger and pediveliger stages. During metamorphosis, muscle structures in the anterior adductor, velum retractors and ventral retractors were degenerated. At the same time, mantle and gill musculature appeared and became the primary muscle system in juveniles together with the posterior adductor. In addition, indirect immunofluorescence with the monoclonal antibody against *C. gigas* muscle proteins (myosin heavy chains (MYHC) and α-actinin) were used to monitor changes in the developing musculature at different larval stages. The immunofluorescence staining results of muscle proteins were consistent with phalloidin staining. The expression locations of two muscle proteins were similar and mainly located in larval velum retractor and adductor muscle. The α-actinin expression positions were located in *Z*-lined of velum striated retractors. Data from these studies provide a comprehensive description of myogenesis in *C. gigas* embryos and larvae. Moreover, our data showed that metamorphosis has a significant impact on remolding the musculature after transition from a mobile planktonic larvae to a sessile mollusk, associated with certain muscle group degradation.

1. Introduction

The Pacific oyster (*Crassostrea giga*) is a sessile bivalve living in the intertidal zone. It is one of the most widely cultivated marine mollusks in the world with a global production of over 4 million tons per year (http://www.fao.org). *C. gigas* has a complex multistep pattern of development, from embryo, larvae, juvenile to adult. During metamorphosrsis, free swimming larvae are transformed to sessile juvenile. The metamorphic transition is tightly linked with changes in the body plan, morphology, habitat and feeding behavior (Evans et al., 2009). An explicit reorganization occurs in the body plan during metamorphosis (Bonar, 1976; Chia and Rice, 1979). As one of the most important organ systems in bivalves, the muscular plays an indispensable role throughout the bivalve lifecycle, and undergoes a dramatic remodeling during metamorphosis. However, little is known about the ontogeny of musculature in Pacific oyster larvae, and especially the dynamic changes of musculature during metamorphosis.

Muscles are vital to bivalve movement, defense and growth. It has been reported that oyster larvae move with the help of cilia and retractor muscles in the veliger stage and crawl with the foot during metamorphosis (Odintsova et al., 2007; Chantler, 2016). By contrast, the adductor muscles in adult bivalves are primarily used to facilitate opening and closing of the valves to protect themselves when a disturbing stimulus or predators are present. The strength of adductor muscle has been used as an indicator of the health condition in bivalve breeding and culture management (Poulet et al., 2003; Fujiwara et al., 2010). In addition to locomotion and protection, bivalve muscles also serve as a metabolic organ that plays a vital role in animal growth. In bivalves, muscles have been implicated in the storage and mobilization of nutrients in order to meet growth requirements (Mathieu and Lubet,

* Corresponding author at: Key Laboratory of Mariculture (Ocean University of China), Ministry of Education, Qingdao 266003, China.
E-mail address: qili66@ouc.edu.cn (Q. Li).

https://doi.org/10.1016/j.cbpb.2018.08.008
Received 26 March 2018; Received in revised form 2 August 2018; Accepted 27 August 2018
Available online 05 September 2018
1096-4959/

1993).

The musculature necessary for adult behavior differs from that in the larvae. During development, bivalves transform from free swimming planktonic larvae to the sessile mollusk through metamorphosis. During the transition, the muscular system changes dramatically from a larval musculature to an adult pattern (Odintsova et al., 2007; Evans et al., 2009). The larval musculature contained mainly adductor and velum retractor muscles, as well as the foot and mantle musculature. In contrast, adductor and mantle muscles are the dominant musculature in adults. It has been shown that *C. gigas* adductor muscles contained two major types, namely the translucent striated muscle for rapid shell closing and the opaque smooth muscle used for holding the shells tightly shut for long periods (Squire, 2012).

While myogenesis has been examined in mollusks such as *Patella*, *Haliotis kamtschatkana*, *Aplysia californica*, *Antalis entails* and *Chaetoderma* (Wanninger et al., 1999; Page, 1997; Wollesen et al., 2008; Wanninger et al., 1999). Myogenesis has only been reported in three species of Bivalvia, including mussel *Mytilus trossulus* (Dyachuk et al., 2012), scallop *Nodipecten nodosus* (Audino et al., 2015) and teredinid shipworm *Lyrodus pedicellatus* (Wurzinger-Mayer et al., 2014). Larval musculature first appeared at the trochophore stage, and the well-organized muscular systems are formed at the veliger stage (Audino et al., 2015). More elaborated musculature is established at the pediveliger stage containing anterior and posterior adductors, velum and foot retractors and mantle muscles (Audino et al., 2015).

To characterize the ontogeny of muscular system in *C. gigas,* we performed phalloidin staining to define the temporal and spatial patterns of actin filaments in key muscle groups during oyster development and metamorphosis. We also investigated the expression patterns of major muscle proteins including MYHC and α-actinin during larval development stages. Data from these studies provide a comprehensive description of myogenesis in *C. gigas* of the larval and early juvenile stages.

2. Methods

2.1. Rearing of animal

Adult *C. gigas* were collected from Laizhou, China and maintained in concrete tanks with aerated, filtered seawater at 20–23 °C. Eggs and sperms were collected from adult pairs and manually fertilized in vitro. After fertilization, the embryos were placed into hatching tanks and reared as described by Kong (Kong et al., 2015). After 24 h incubation, larvae were collected from hatching tanks and stocked into larval rearing tanks. Water temperature was maintained at 23–24 °C, with salinity at 30 psu. The tank water was exchanged at 50% twice daily and 100% every 10 days. Veliger larvae were fed with algal diet of *Isochrysis galbana* until the larvae reached 120 μm in shell length, then fed with *Platymonas helgolandica* and *Chaetoceros calcitrans* at later stages. Larvae were fed at concentrations ranging from 30,000 to 80,000 cells/ml, depending on age. When larvae at a size of 320–340 μm were observed, spat collectors (strings of scallop shells) were placed in the tanks. After a week, successfully metamorphosed spat were transferred to outdoor nursery tanks. Samples were collected at the following stages: fertilized egg, blastula, gastrulae, trochophore, veliger, pediveliger, postmetamorphic and juvenile.

2.2. Sample preparation and F-actin staining

Samples were anesthetized with 7.5% $MgCl_2$, and then fixed in 4% paraformaldehyde (PFA) in 0.1 M phosphate buffered saline (PBS, pH = 7.3) for 2–3 h at room temperature (RT). Afterwards, the larvae were washed three times for 10 min each in PBS at RT and then were stored at 4 °C in PBS with 0.1% NaN_3. Decalcification was performed in 0.2 M ethylene diamine tetraacetic acid (EDTA) for 10–20 h at RT. EDTA solution was displaced by washing the samples thrice for 15 min each in 1xPBS. All specimens were permeabilized in PBS containing 2% Triton-X 100 (PBT, pH = 7.3) overnight. Staining of musculature was performed by fluorescence labeling of filamentous F-actin with Phalloidin-iFluor™ 488 Conjugate (AAT Bioquest) in a 1:1000 dilution in PBT for 24 h in the dark. Subsequently, the samples were rinsed three times for 15 min each in 1xPBS and then mounted in Fluoromount G (Southern Biotech) between two coverslips to allow scanning from both sides.

2.3. Western blotting

Frozen striated and smooth adductor muscles were dissolved in SDS-extracting solution (2% SDS, Tris-HCl (pH 6.8), 2% β-mercaptoethanol, 25% glycerol). The homogenates were centrifuged at 12000 ×*g* at 4 °C for 30 min. The supernatant was mixed with 4× protein loading buffer, 100 °C boiled for 10 min, and stored at −20 °C. SDS-PAGE was carried out using 12% (α-actinin) and 6% (MYHC) polyacrylamide gel and a discontinuous Tris-glycine buffer system. Protein bands were detected by staining with Coomassie R250 (Solarbio). For western blotting, the proteins were transferred electrophoretically from the polyacrylamide gel to a PVDF membrane in a towbin buffer containing 20 mM Tris-HCl (pH 8.0), 192 mM glycine, 20%(*v*/v)methanol. The PVDF membrane was blocking with 5% bovine serum (BSA) in TTBS buffer (20 mM Tris-HCl (pH 7.5), 500 mM NaCl, 0.05% Tween 20) and then incubated in primary antibodies including MYHC (DSHB) and α-actinin (DSHB) overnight at 4 °C, followed by incubated in AP-labeled second antibodies (1:500) overnight at 4 °C. The protein bands were then treatment with NBT/BCIP solution for 10 min in darkness at room temperature. Color development was stopped by Milli-Q water.

2.4. Immunochemistry

Method of sample fixation and preservation were same to F-actin staining. In order to obliterate nonspecific binding, samples were incubated overnight at 4 °C in a blocking buffer including 5% serum albumin (Solarbio), 2% Triton X-100 and 0.03% NaN_3. Samples were incubated with the primary antibodies against MYHC (DSHB, 1:10) and α-actinin (DSHB, 1:10) in the blocking buffer at 4 °C for two days. Samples then were washed three times for 15 min each in 1xPBST. FITC-labeled goat anti-mouse antibodies (1:500) in blocking buffer were used as the second antibodies. In parallel, Phalloidin-iFluor™ 488 Conjugate (AAT Bioquest) was added to the incubation medium. Samples were incubated in second antibodies overnight at 4 °C, and then rinsed three times in 1× PBST for 15 min. The fluorescence microscope was used to collect pictures.

2.5. Confocal microscopy and 3D reconstruction

Image acquisition and analysis were performed on a Nikon ECLIPSE Ti confocal laser scanning microscope equipped with the software NIS-Elements (Version 4.0). Confocal image stacks were recorded with 0.2–0.4 μm step size along the z-axis and digitally merged as maximum intensity projections. The confocal stacks were manipulated with the 3D-reconstruction software Imaris 7.2 (Bitplane) and Mimics (Materialise) to obtain the 3-dimensionality of the larvae.

2.6. Orientation and nomenclature of larvae

Controversial theories exist concerning the axis determination and orientation in bivalve larvae. This is primarily due to the fact that the morphological dorsoventral designation used in adult bivalves has been applied to define the orientation in the (pedi-) veliger stages (Wurzinger-Mayer et al., 2014). In this study, identification of larval body axes and orientation were used in conformity to comparative lophotrochozoan larval anatomy (Wanninger, 2009). In larvae, the position of the apical tuft was referred as the anterior and ventral side

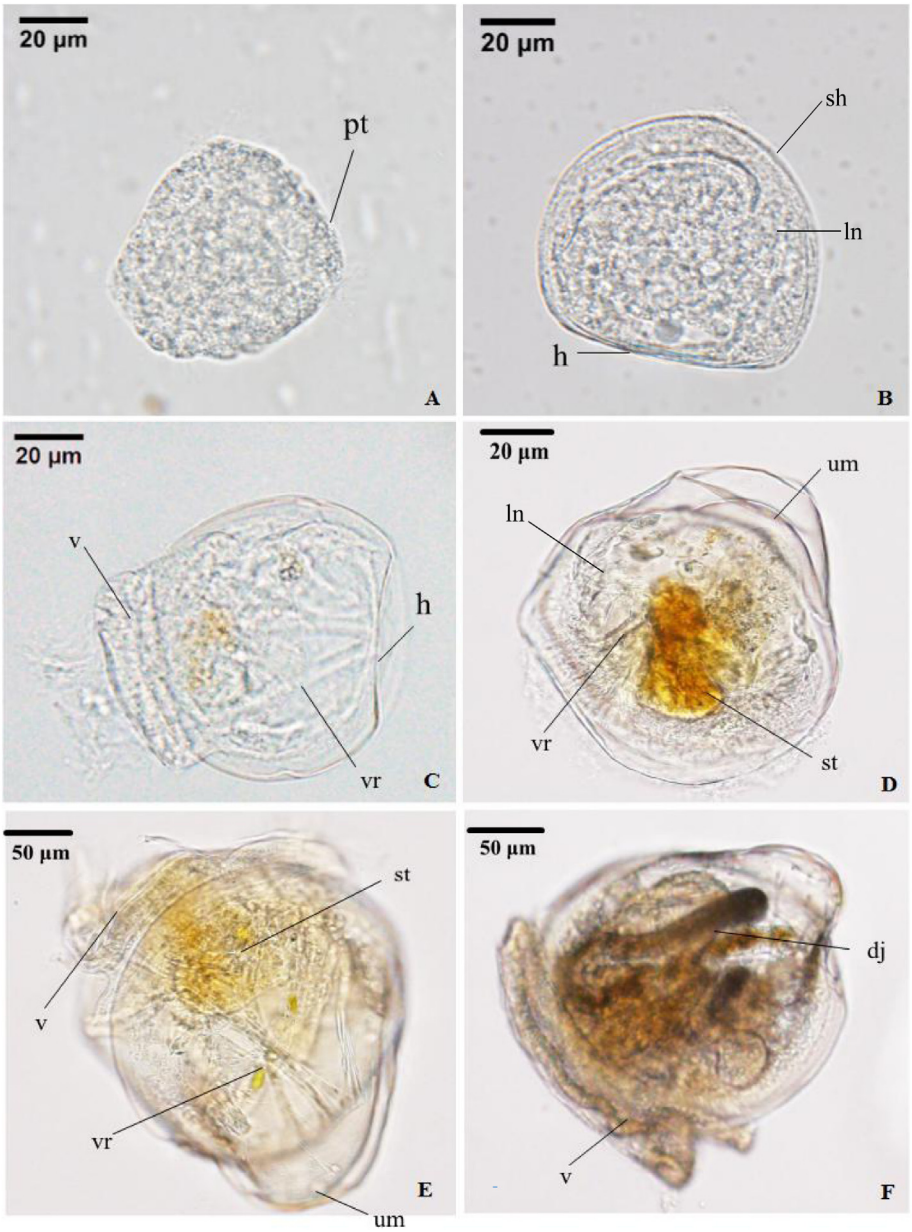

Fig. 1. The stages of ontogenesis in *C. gigas*. (A) Late trochophore (16 h post fertilization [hpf]) (B) Early veliger with an extending anlage of the shell (48 hpf) (C) D-shaped larvae stage (24 hpf). (D) Late veliger stage (10 days post fertilization [dpf]). (E) Pediveliger stage (15 dpf). (F) Postmetamorphic stage (20 dpf). h:hinge; ln: intestine; um: umbo; vr: velum retractor; st: stomach; dj: digestive; v: velum;

while the opposite of apical tuft was identified as the posterior and dorsal side. In the veliger larvae, the hinge region was designated as the posterior and the velum region was referred as the anterior. In post-metamorphic and adult bivalves, the axis from mouth to anus marked ventral and anterior, respectively. The shell hinge represented the dorsal and posterior side.

3. Results

3.1. Characterization of embryonic and larval development in C. gigas

The embryonic and larval development was characterized in *C. gigas* from fertilization to approximately one month post-fertilization. It includes the following developmental stages, namely trochophore, D-shaped, veliger, pediveliger and postmetamorphic stages (Fig. 1). The fertilized eggs developed into a free-swimming trochophore in approximately 12 h (Fig. 1A). At the early veliger stage (24–48 h), the larvae formed shell rudiment and gradually became "D-shaped" (Fig. 1B). The larvae at the late veliger stage (3–10 days) possessed disk shaped velum (Fig. 1C, D). The veliger then developed into pediveliger (11–20 days) which had a remarkable umbo on the larval shell (Fig. 1E). When pediveliger developed into post-metamorphic larvae (20–25 days), the larvae possessed a pigmented eyespots (Fig. 1F). Then after 5–7 days, the larvae metamorphosed to spats.

3.2. Musculature of C. gigas larvae at trochophore and veliger stages

To characterize the temporal and spatial patterns of myogenesis in *C. gigas*, we analyzed actin filaments at several developmental stages using phalloidin staining and confocal microscopy. Our data revealed that there was little or no muscle specific phalloidin staining in fertilized egg, blastula and gastrula stage embryos (Data not shown). The first larval musculature appeared at the early trochophore stage. In this stage, a noticeable "U-shaped" muscle ring emerged at the vegetal pole

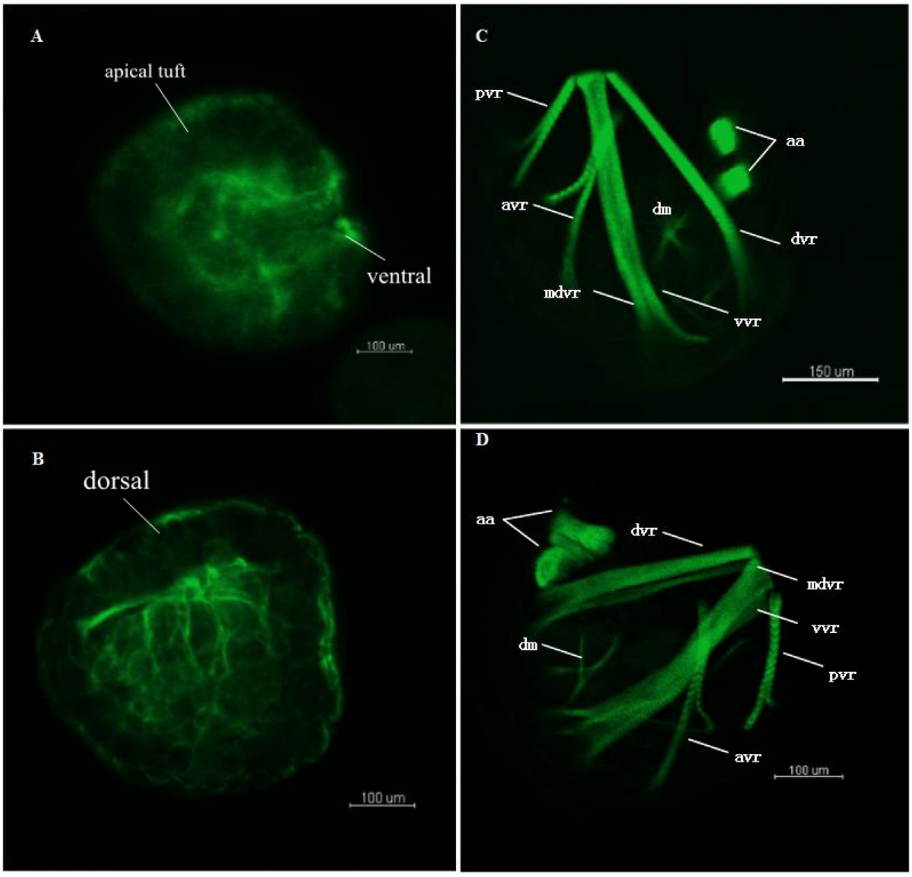

Fig. 2. Myogenesis from early trochophore to the "D"-shape stage in *C. gigas* (confocal micrographs). All aspects were in lateral view. (A) larval musculature in early trochophore stage (12 hpf). (B) larval musculature in late trochophore stage (18 hpf). (C) larval musculature in "D"-shape stage (24 hpf). (D) larval musculature in "D"-shape stage (48 hpf). Abbreviations: aa, anterior adductor; dm, digest musculature; dvr, dorsal velum retractors; mdvr, medio-dorsal velum retractors; vvr, ventral velum retractors; avr, anterior ventral retractors; pvr, posterior ventral retractors.

of the larvae (Fig. 2A). When larvae developed into the late trochophore stage, several muscle bundles were detected at same position of the initial muscle ring. These muscle bundles represent the rudimentary muscle structure of the *C. gigas* larvae (Fig. 2B).

As the embryo developed into D-shaped and veliger larvae, a complex musculature was observed that consisted of various muscle groups. In the early veliger larvae, "D-shaped" shell was newly formed and this was accompanied with the appearance of anterior adductor muscle (Fig. 2C-D). The anterior adductor muscle was divided into two parts which were stretched across the left and the right valves. The adductor muscle and velum retractor muscle became a significant part of the musculature system (Fig. 2C-D).

In addition to the adductor muscles, other prominent muscle groups included the larval velum retractor and ventral retractor muscles (Fig. 3A-C, Fig. 5A-a). The larval velum retractors were responsible for retraction of the velum into the pallial cavity. The larval velum retractors constituted of three branched muscle pairs containing exclusively striated myofibers (Fig. 3A-C, Fig. 5A-a). These velum retractors were attached to the hinge and distributed on both sides of the body. A pair of dorsal velum retractors attached to the developing shell, which extended anteriorly into the velum and ran along the anterior adductor (Fig. 3A-C, Fig. 5A-a). The medio-dorsal velum retractors with many branches were medially attached to the velum. Clearly distinct from the dorsal velum retractors, a pair of ventral velum retractors appeared running into the velum (Fig. 3A-C, Fig. 5A-a). In addition, the ventral velum retractors with plenty of branching crossed the body obliquely along the larval dorsa-ventral axis. Moreover, two pairs of muscle bundles named the ventral larval retractors appeared at this stage and attached to a more ventral region of the larvae (Fig. 3A-C, Fig. 5A-a). The ventral larval retractors composed of striated muscle fibers became two muscle bundles before attaching to the ventral body wall (Fig. 3B-C). Furthermore, the anterior ventral retractors ran toward the ventral side from the upper part of the ventral velum retractors whereas the posterior ventral larval retractors stemmed from the base of the velum retractors (Fig. 3A-C, Fig. 5A-a).

A few thin muscle bundles made up of transparently smooth fibers were present at the intermediate position of the digestive tract. In late veliger stage, there was few conspicuous change compared to the early veliger stage except that the appearance of the posterior adductor anlage which stemmed from the terminal of the ventral velum retractors (Fig. 3A-C, Fig. 5A-a).

3.3. Musculature of *C. gigas* larvae in the pediveliger stage

A dramatic increase in size and number of larval musculature was detected at the pediveliger stage (Fig. 3D-E, Fig. 5B-b, Fig. 5C-c). The posterior adductor became more massive and well-development. The posterior adductor appeared at the position near the inner surface of the shell and attached to the left and right valves. Differing from the anterior adductor, the posterior adductor consisted of several muscle bundles. The anterior and posterior adductors connected the left and right valves and controlled the open or close of the larval shell. The velum retractors became intensely branched, while the original pairs disappeared at this stage. The ventral and dorsal velum retractors became denser, and split apart into a large number of branches. In the meantime, these branches ran into the velum where the branches spread out. In contrast to these visible changes in velum retractor development, the ventral retractors showed no visible changes at this stage.

Furthermore, some novel muscle groups were present in foot retractor muscles at the pediveliger stage. The foot retractors appeared in a cruciform shape. There were two different infusion sites of the foot retractors originated from the medio-ventral region and posterior adductor regions, respectively. At the late pediveliger stage, the margin-

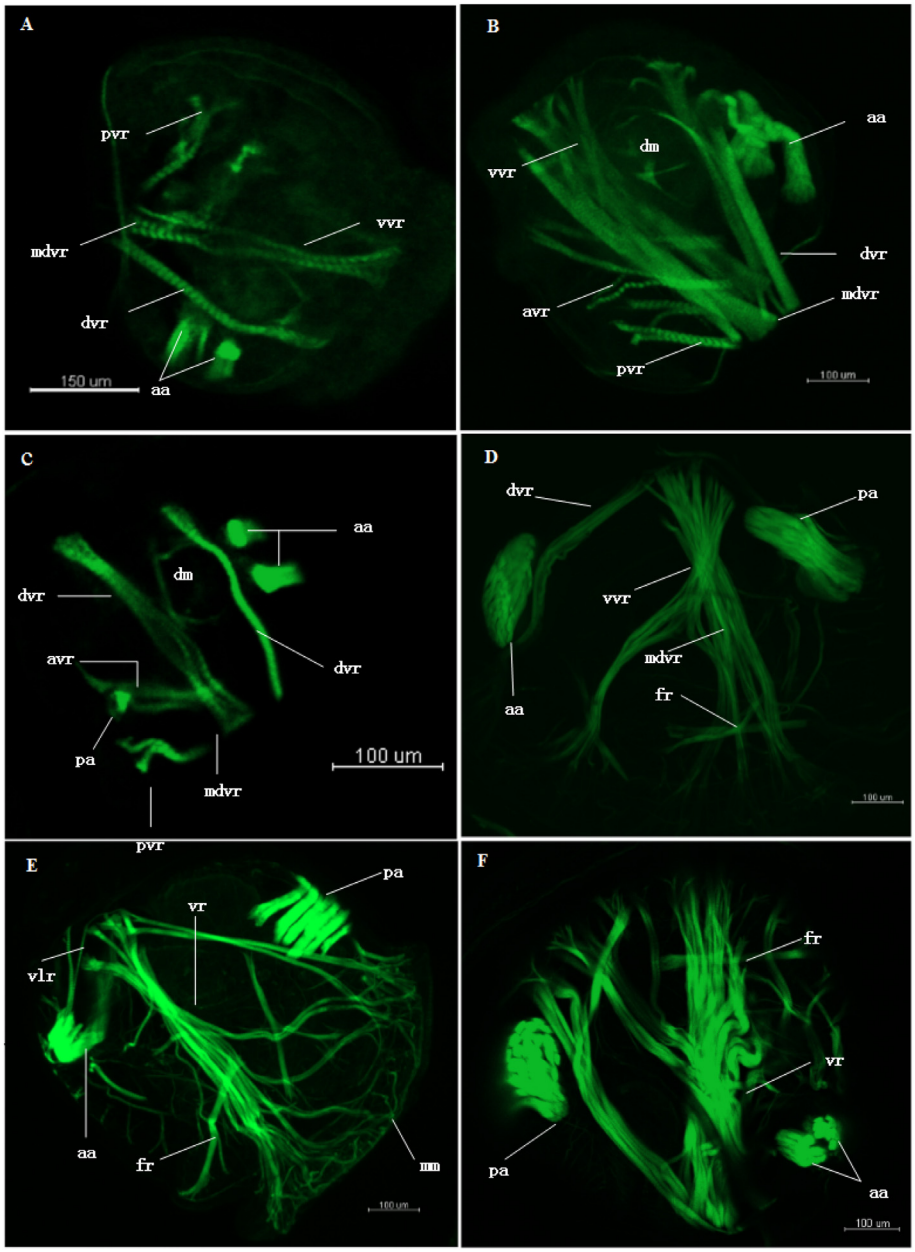

Fig. 3. Musculature of *C. gigas* larvae in the veliger stage (confocal micrographs). All aspects were in lateral view. (A) larval musculature in veliger stage (3 days post fertilization [dpf]). (B) 3D Confocal image of larval musculature in veliger stage (5 dhf). (C) larval musculature in veliger stage (7 dhf). (D) Confocal micrograp of larval musculature in early pediveliger stage (10 dhf). (E) larval musculature in middle pediveliger stage (15 dhf). (F) larval musculature in late pediveliger stage (18 dhf). Abbreviations: aa, anterior adductor; pa, posterior adductor; dm, digest musculature; dvr, dorsal velum retractors; mdvr, medio-dorsal velum retractors; vvr, ventral velum retractors; avr, anterior ventral retractors; pvr, posterior ventral retractors; fr, foot retractors; mm, mantle muscle.

parallel muscle appeared (Fig. 3F, Fig. 5D-d). The mantle margin exhibited muscles running along its extension.

3.4. The effect of metamorphosis on muscle development

Once the larvae possessed the eyespots, they entered the post-metamorphic stage and started to enact the settlement gradually. In the early post-metamorphic stage, the anterior adductor still existed and had no obvious alteration apart from the increase in size. The posterior adductor, on the other hand, became well-developed and more massive than the anterior adductor (Fig. 4A, Fig. 5E-e). As metamorphosis progressed, the velum retractor muscles came away from the shell edge and started to degenerate. The dorsal and ventral velum retractors became thicker and no longer attach to the velum. The ventral retractors shed in this stage. The dorsal and ventral velum retractors gradually integrated into the larval mantle and become part of the future mantle musculature (Fig. 4B-D). The mantle margin ran along the shell edge and contained muscles in two major patterns. The margin-parallel muscle projected in a pattern parallel to the edge of the mantle, whereas the vertical muscle bundles attached to the shell and ran into the mantle margin.

In the late post-metamorphic stage (Fig. 4E-F), the adductor, mantle and foot muscle systems became the dominant musculature. The juveniles possessed a large posterior adductor while the anterior adductor was under degeneration. The foot musculature only possessed one attachment site near the posterior adductor and the other insert position was lost. The foot musculature became more complex consisting of foot retractors and pedal plexus. The foot retractors and pedal plexus were the primary components of the foot muscle systems. The foot retractors originated from the medio-ventral of the body and the pedal plexus was positioned at the end of the foot retractors. The foot retractors contained muscle fibers attached to the shell while the pedal plexus consisted of thin muscle bundles in the terminal region of the foot (Fig. 4D-E).

3.5. The musculature in juvenile C. gigas

Juvenile attained the characteristics of adult morphology after

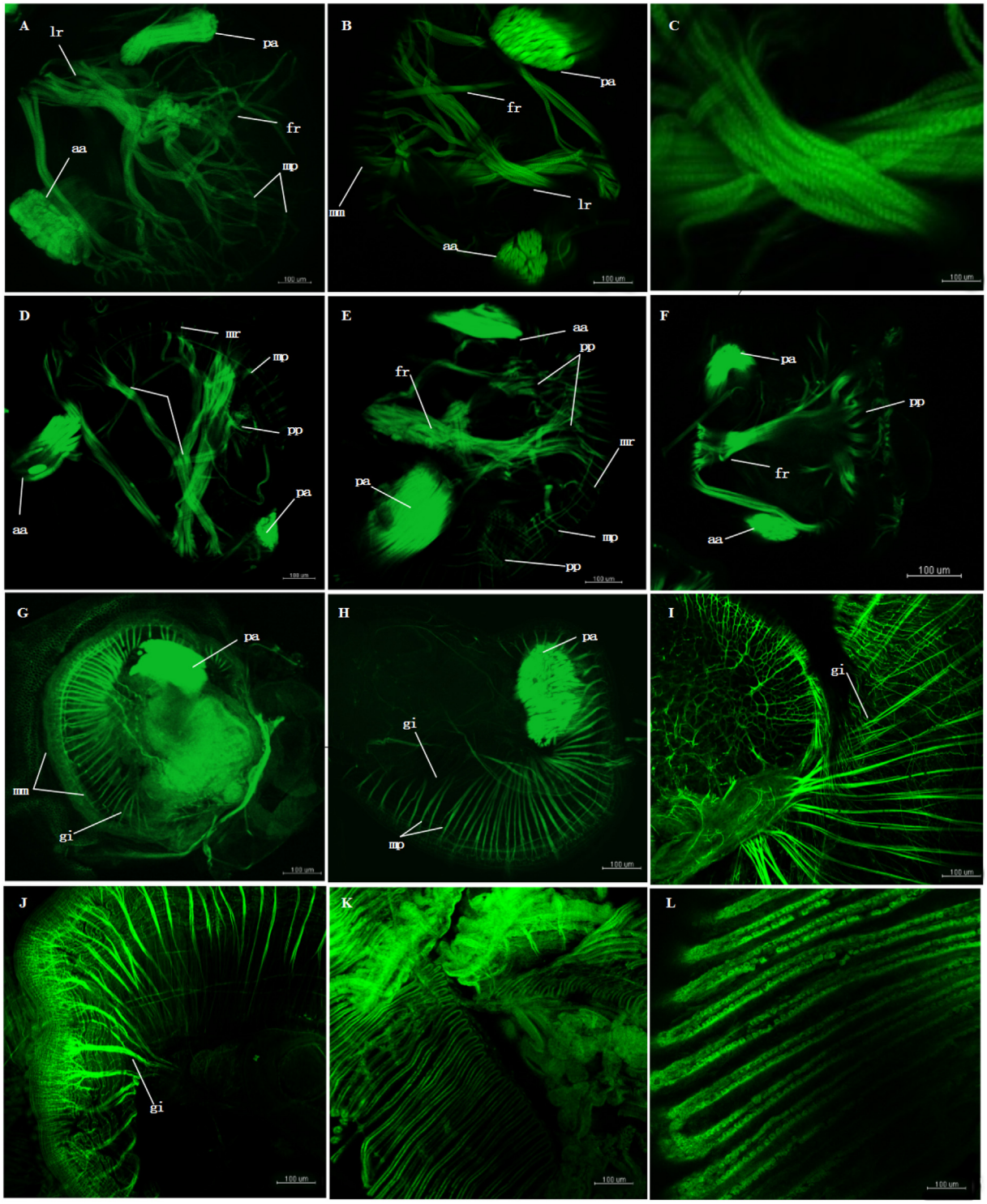

Fig. 4. Musculature of *C. gigas* larvae in post-metamorphic and juvenile stage (confocal micrographs). All aspects were in lateral view. (A) 3D confocal image stacks of larval musculature in early post-metamorphic stage (20 dpf). (B) 3D confocal image stacks of larval musculature in middle post-metamorphic stage (22 dpf). (C) Larval striated retractors in middle post-metamorphic stage (22 dhf). (D) Larval musculature in middle post-metamorphic stage (25 dpf). (E) larval musculature in middle-late juvenile stage (28dpf). (F) larval musculature in late juvenile stage(31dpf). (G) larval musculature in late juvenile stage (7 days after settlement). (H) larval musculature in late juvenile stage (10 days after settlement). (I) larval musculature in late juvenile stage (15 days after settlement). (J-L) gill muscle in late juvenile stage (15 days after settlement). Abbreviations: aa, anterior adductor; pa, posterior adductor; fr, foot retractors; pp., pedal plexus; mp, mantle margin-parallel muscle; mr, mantle retractors; gi, gill.

adhered for five days on the settlement. Our data revealed that the posterior adductor, mantle and gill became the prominent musculaturein the juveniles (Fig. 4E-F, Fig. 5F-f). The juveniles met the monomyarian requirement by possessing only the posterior adductor with the anterior adductor completely degenerated. The posterior adductor was well-developed and connected the left and right shells. The mantle retractors were also well-developed and had no visible changes compared to the previous stage. The margin-parallel muscle increased

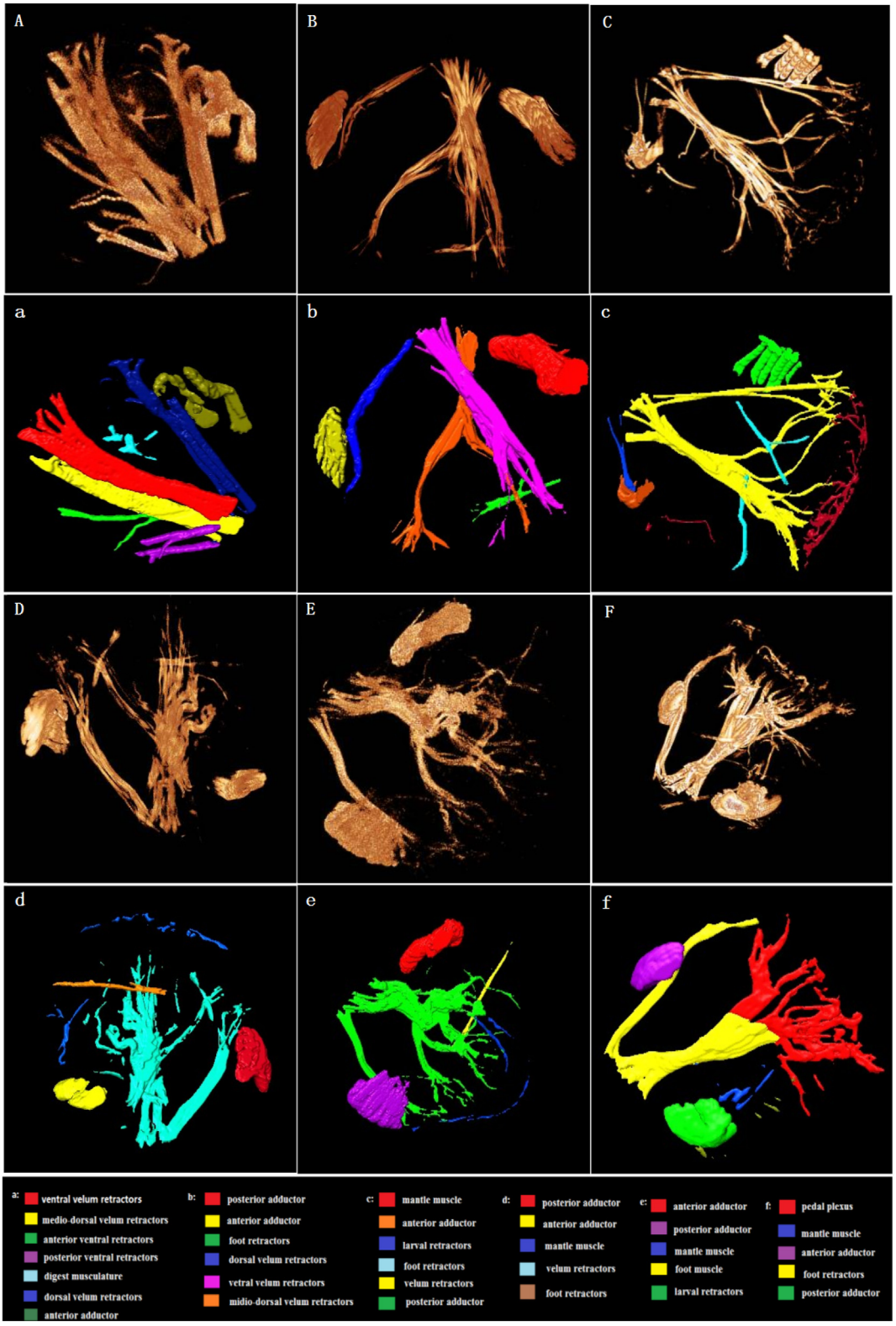

Fig. 5. 3D reconstructions of the muscular architecture from veliger to post-metamorphic stage of *C. gigas*. Reconstructions are based on the confocal microscopy dataset shown in Fig.3 and Fig. 4. (A-a) larval musculature in early veliger stage. (B-b) larval musculature in early pediveliger stage (10 dhf). (C-c) larval musculature in middle pediveliger stage (15 dhf). (D-d) larval musculature in late pediveliger stage (18 dhf). (*E*-e) larval musculature in early post-metamorphic stage (20 dpf). (F-f) larval musculature in late juvenile stage (15 days after settlement).

in size and extended along the edge of the shell. The gill musculature appeared at the middle parts of the body (Fig. 4G-I). The gill filaments were curved inward forming a “gill basket” within the mantle cavity. The filaments generated large number of branches in the distal extremities and these branches intertwined with each other (Fig. 4J-L). Furthermore, more thin muscle bundles appeared at the digestive gland position, and the foot musculature of juveniles were completely degenerated.

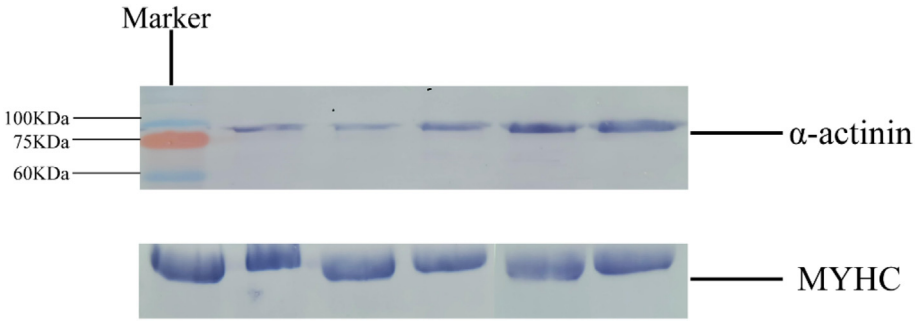

Fig. 6. Western blotting analysis of antibody against MYHC and α-actinin prtotein.

3.6. Protein localization patterns of MYHC and α-actinin

Western blotting was performed to determine the protein expression level of MYHC and α-actinin. Specificity of the Abs against the muscle proteins of the MYHC and α-actinin was tested by WB (Fig. 6). The specific single strand was located in the corrected location where was consistent with the protein molecular weight, suggesting that the antibodies against MYHC and α-actinin were specific and applicative. Immunofluorescence was used to identify the expression location of proteins. We found that the expression location of MYHC and α-actinin by indirect immunofluorescence was similar to the arrangement of actin filaments by phalloidin staining (Fig. 7). The muscle proteins were major located in larval velum retractors and larval retractors during veliger and eyed larval stage. The expression positions of α-actinin were located in *Z*-lined of velum striated retractors and larval retractors. In addition, the specificity and accuracy of Phalloidin staining were stronger than immunofluorescence staining in visualization of larval myogenesis progress (Fig. 7I-J).

4. Discussion

In this study, we analyzed myogenesis in *C. gigas.* Our data revealed a dynamic pattern of musculature in pacific oyster during early development and metamorphosis. A simple U-shaped muscle ring first appeared at the trochophore stage. This was followed by a more complex musculature at the veliger and pediveliger stages. The musculature underwent a dramatic reorganization during metamorphosis.

Data from our studies also provide the basis for comparative analysis of muscle development in Bivalvia. Several similarities and differences were observed in the muscular systems among bivalves. The similarities and differences in musculature could reflect the evolutionary relationship among bivalve species. For example, bivalve species with the appearance of the anterior adductor prior to the posterior adductor and the degeneration of anterior adductor, larval velum retractors and foot musculature during metamorphosis could suggest that these species might came from the common ancestor.

4.1. Adductor musculature

In *C. gigas*, the anterior adductor developed in the early veliger stage and the posterior adductor appeared in the late veliger stage. This is consistent with the general finding in bivalves that the anterior adductor is formed prior to the posterior adductor (Altnoeder and Haszprunar, 2008). The posterior adductor stemmed from the ventral velum retractors in *C. gigas* and the phenomenon also occur in L. *pedicellatus* (Wurzinger-Mayer et al., 2014). The anterior adductor was well-developed than the posterior adductor at the early veliger stage while the posterior adductor became more massive at the late veliger stage in *C. gigas*. This phenomenon also occurred in other bivalves including *Aequipecten irradians* (Sastry, 1965), *Argopecten purpuratus* (Bellolio et al., 1993), *N. nodosus (*Audino et al., 2015), *M. trossulus* (Dyachuk and Odintsova, 2009) and *Ostrea edulis* (Cole, 1938). The anterior adductor was divided into two portions in *C. gigas*, and this is similar to the *Pecten.maximus* (Cragg, 1985), scallop *N. nodosus* (Audino

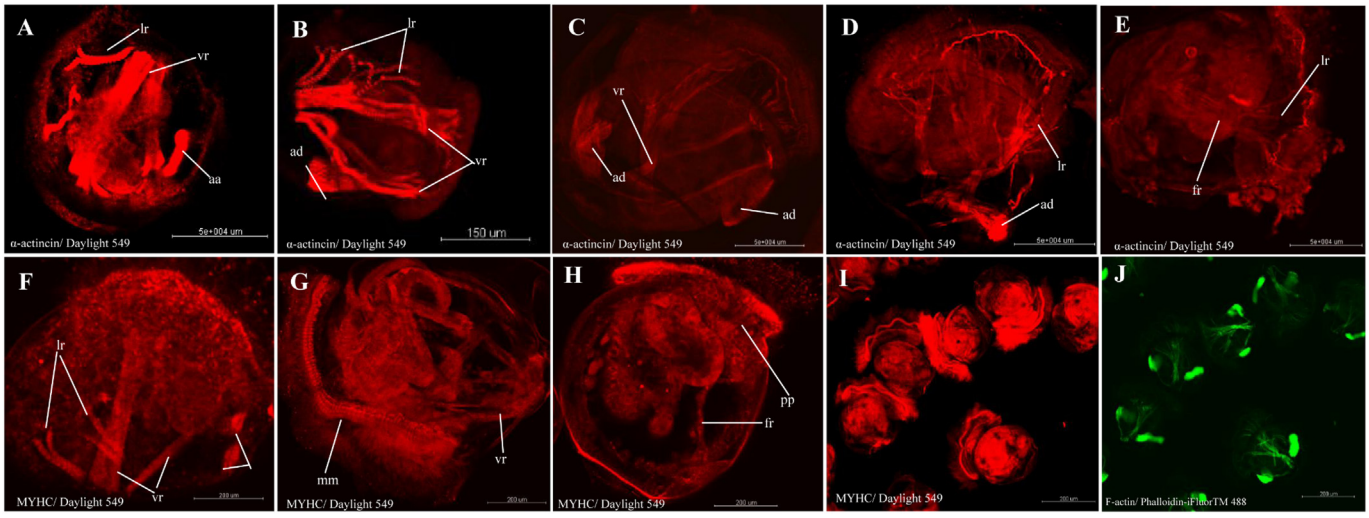

Fig. 7. Indirect immunofluorescence with the monoclonal antibody against MYHC and α-actinin. (A-E) MYHC immunoreactivity at larval different development stage. (F—H) α-actinin immunoreactivity at larval different development stage. (I-J) larvae were double-labeled with MYHC (red) and phalloidin (green). vr: velum retractor; ad: adductor muscle; lr: larval retractor; mm: mantle; fr: foot retractors; pp.: pedal plexus. (For interpretation of the references to color in this figure legend, the reader is referred to the web version of this article.)

et al., 2015) and *M. trossulus* (Dyachuk and Odintsova, 2009). The posterior adductor in *C. gigas* larvae consisted of several muscle bundles, which was different from the scallop larvae which posterior adductor was divided into two parts. In L. *pedicellatus* the posterior adductor also appeared to be divided into multiple muscle units (Wurzinger-Mayer et al., 2014). Furthermore, In *C. gigas,* the adult possessed a monomyarian arrangement with only one adductor while the larvae had the dimyarian condition. The larvae had both anterior adductor and posterior adductor, of which the anterior adductor degenerated during the metamorphosis stge. Moreover, the same pattern was found in other bivalves such as *N. nodosus*, *M. trossulus* and *Ostrea edulis* (Audino et al., 2015; Dyachuk and Odintsova, 2009; Cole, 1938). Not all of bivalves like this, the dimyarian condition has already established in the larvae of L. *pedicellatus* and kept the same in the adults (Wurzinger-Mayer et al., 2014).

4.2. Larval retractors systems

The retractor systems have been investigated in detail in larval musculature of bivalve and diverse findings were obtained in those species examined (Wurzinger-Mayer et al., 2014). The major difference included the number of retractors and the timing of emergence and degeneration. Similar to *M. trossulus, Lasaea adansonii* and *Pandora inaequivalvis*, *C. gigas* had three pairs of velum retractors from the onset of myogenesis (Dyachuk and Odintsova, 2009; Altnoeder and Haszprunar, 2008; Allen, 1961). In contrast, four pair of velum retractors were found in scallop *N. nodosus*, *P. maximus*, *Tridacna maxima* and *Tridacna crocea* (Audino et al., 2015; Cragg, 1985; La Barbera, 1975; Jameson, 1976). *L. pedicellatus* had two pairs of velum retractors (Wurzinger-Mayer et al., 2014).

C. gigas had two pairs of shell-anchored larval ventral retractors in veliger stage and a pair of larval ventral retractors appeared at pediveliger and veliger stages. Similar system was also found in *N. nodosus*, *P. maximus*, *M. trossulus* (Audino et al., 2015; Cragg, 1985; Dyachuk and Odintsova, 2009). Like the *N. nodosus*, the larval velum retractors of *C. gigas* appeared at the early veliger stage and disappaered at the late postmetamorphic stage (Audino et al., 2015). However, the velum retractors did not degenerate until the pediveliger stage in *M. trossulus* and *P. maximus* (Dyachuk and Odintsova, 2009; Cragg, 1985). In L. *pedicellatus*, the velum retractors appeared at the early veliger stage and never shed (Wurzinger-Mayer et al., 2014). The ventral larval retractors in *C. gigas* disappeared in the late postmetamorphic stage and this phenomenon was also found in *N. nodosus* (Audino et al., 2015). The ventral retractors in *Dreissensia polymorpha* was maintained until late veliger stage (Bellolio et al., 1993). Similar to *N. nodosus* and *M. trossulus*, the larval retractors was striated muscle in *C. gigas* (Wanninger et al., 1999; Wurzinger-Mayer et al., 2014).

4.3. Larval foot musculature

In *C. gigas*, we speculated that the foot retractors originated from the velum retractors because the insertion sites of the foot retractors. The foot retractors had two different insertion sites formed at the medioventral region and posterior adductor region, respectively. It has been reported that the foot of *N. nodosus* and L. *pedicellatus* originated from larval velum retractors (Wanninger et al., 1999, Wurzinger-Mayer et al., 2014). The foot retractors firstly presented a pattern called cruciform retractors at the pediveliger stage and this phenomenon was also observed in *Ostrea edulis* (Cole, 1938). Interestingly, the pedal plexus of *C. gigas* possessed two different patterns at the late post-metamorphic stage. One presented a complex muscular grid and the other consisted of thin muscle bundles. The grid muscle pattern also occurred in L. *pedicellatus* foot musculature (Wurzinger-Mayer et al., 2014). The foot pedal plexus of *N. nodosus* showed a disorganized pattern made up of thin muscle bundles (Audino et al., 2015). The foot musculature of *C. gigas* first appeared in the pediveliger stage and degenerated at the adult stage. In *C. gigas*, the foot muscle systems shed in the juvenile stage while the foot musculature was still present in *M. trossulus* and *N. nodosus*. We speculate that this might be determined by their different living habit (Dyachuk and Odintsova, 2009; Wurzinger-Mayer et al., 2014).

4.4. Mantle musculature

We showed in this study that in *C. gigas*, the mantle margin-parallel muscles first appeared at the late pediveliger stage and the mantle retractors were formed at the post-metamorphic stage. Compared with previous findings from other bivalves, it is evident that timing of the appearance of mantle muscle systems differs among bivalves. In *N. nodosus*, the mantle musculature including margin-parallel muscles and mantle retractors appeared at the same time in the pediveliger stage (Audino et al., 2015). In contrast, formation of mantle musculature occurred at the late veliger stage in *M. trossulus* (Dyachuk and Odintsova, 2009).

4.5. Gill musculature

As in *P. maximus*, we showed that *C. gigas* juveniles had the gill musculature until it adhered for several days (Cragg, 1985). In *C. gigas*, the gill filaments formed a “gill basket” within the mantle cavity and the filaments generated many branches in the terminal region. Similarly, juveniles had gill muscles with numerous branching thin muscle fibers in *M. trossulus* (Dyachuk and Odintsova, 2009). Gill musculature consists of three distinct groups: longitudinal, dorso-ventral, and water tube muscles in bivalves (Gainey, 2010). We speculated that the juvenile gill muscle filaments that elongated radially from the center of the body could develop into future longitudinal muscles. The branches in the terminal of the filaments would develop into future tube muscles.

4.6. Protein localization patterns

Muscle is composed of thick and thin filament. F-actin and α-actinin are major component of thin filament, and MYHC is chief component of thick filament. We found that the expression location of MYHC and α-actinin by indirect immunofluorescence was similar to the arrangement of actin filaments by phalloidin staining. However, we thought indirect immune-whole larval staining of some muscle proteins have an inevitable non-specific staining especially for species which own shell and valve. It was quite possible to because the monoclonal antibody purchasing from the market was from rabbit species not *C. gigas*. By contrast, phalloidin is a useful tool for investigating the distribution of F-actin in cells by labeling phalloidin with fluorescent analogs and using them to stain actin filaments for light microscopy in many species (Capani et al., 2001). Phalloidin binds to both large and small F-actin with high affinity but, unlike antibodies, does not bind monomeric globular actin (Wulf et al., 1979). In general, we thought fluorescent phalloidin was the most effective ways for the visualization of larval myogenesis progress in terms of specificity and accuracy.

Acknowledgements

This study was supported by the grants from National Natural Science Foundation of China (31772843), Shandong Province (2017LZGC009), the Fundamental Research Funds for the Central Universities (201762014), and Taishan Scholars Seed Project of Shandong. Open Project Program of Laboratory for Marine Fisheries Science and Food Production Processes, Qingdao National Laboratory for Marine Science and Technology (2016LMFS-A06).

References

Allen, J.A., 1961. The development of *Pandora inaequivalvis* (Linne). J Embryol Exp

Morph. 9, 252–268.
Altnoeder, A., Haszprunar, G., 2008. Larval morphology of the brooding clam *Lasaea adansonii* (Gmelin, 1791) (Bivalvia, Heterodonta, Galeommatoidea). J. Morphol. 269, 762–774.
Audino, J.A., Marian, J.E.A.R., Kristof, A., Wanninger, A., 2015. Inferring muscular ground patterns in Bivalvia: Myogenesis in the scallop *Nodipectn. nodosus*. Front. Zool. 12, 34.
Bellolio, G., Lohrmman, K., Dupré, E., 1993. Larval morphology of the scallop *Argopecten purpuratus* as revealed by scanning electron microscopy. Veliger 36, 322–342.
Bonar, D.B., 1976. Molluscan metamorphosis: a study in tissue transformation. Am. Zool. 16, 573–591.
Capani, F., Martone, M.E., Deerinck, T.J., Ellisman, M.H., 2001. Selective localization of high concentrations of F-actin in subpopulations of dendritic spines in rat central nervous system: a 3-dimensional electron microscopic study. J. Comp. Neurol. 435, 156–170.
Chantler, P.D., 2016. Scallop adductor muscles: structure and function. Dev. Aquac. Fish. Sci. 40, 161–218.
Chia, F.S., Rice, M.E., 1979. Settlement and metamorphosis of marine invertebrate larvae. Q Revbiol. 301–302.
Cole, H.A., 1938. The fate of the larval organs in the metamorphosis of *Ostrea edulis*. J. Mar. Biol. Assoc. UK 22, 469–484.
Cragg, S.M., 1985. The adductor and retractors muscles of the veliger of *Pecten maximus* (L) (Bivalvia). J. Molluscan Stud. 51, 276–283.
Dyachuk, V.A., Odintsova, N.A., 2009. Development of the larval muscle system in the mussel *Mytilus trossulus* (Mollusca, Bivalvia). Develop. Growth Differ. 51, 69–79.
Dyachuk, V., Wanninger, A., Voronezhskaya, E., 2012. Innervation of bivalve larval catch muscles by serotonergic and FMRFamidergic neurons. Acta Biol. Hung. 63, 221–229.
Evans, C.C.E., Dickinson, A.J.G., Croll, R.P., 2009. Major muscle systems in the larval *caenogastropod, Ilyanassa obsoleta*, display different patterns of development. J. Morphol. 270, 1219–1231.
Fujiwara, T., Aoki, H., Ishikawa, T., Atsumi, T., 2010. Simple selection of pearl oysters *Pinctada fucata martensii* with strong shell-closing strength using near-infrared spectroscopy. Aquaculture 58, 253–259.
Gainey, L.F., 2010. Seasonal potentiation of gill muscle contraction in four species of bivalve molluscs. J Exp Mar Bio Ecol. 391, 43–49.
Jameson, S.C., 1976. Early life history of the giant clams *Tridacna crocea* Lamarck, *Tridacna maxima* (R?Ding), and *Hippopus hippopus* (Linnaeus). Pac. Sci. 30, 219–233.
Kong, N., Li, Q., Yu, H., Kong, L.F., 2015. Heritability estimates for growth-related traits in the Pacific oyster (*Crassostrea gigas*) using a molecular pedigree. Aquac. Res. 46, 499–508.
La Barbera, M., 1975. Larval and post-larval development of the giant clams *Tridacna maxima* and *Tridacna squamosa* (Bivalvia: Tridacnidae). Malacologia 15, 69–79.
Mathieu, M., Lubet, P., 1993. Storage tissue metabolism and reproduction in marine bivalves—a brief review. Invertebr. Reprod. Dev. 23, 123–129.
Odintsova, N.A., Dyachuk, V.A., Karpenko, A.A., 2007. Development of the muscle system and contractile activity in the mussel *Mytilus trossulus* (Mollusca, Bivalvia). Russ. J. Dev. Biol. 38, 190–196.
Page, L.R., 1997. Larval shell muscles in the abalone *Haliotis kamtschatkana*. Biol. Bull. 193, 30–46.
Poulet, S.A., Lennon, J.F., Plouvenez, F., Jalabert, F., Correc, G., Cueff, A., Lacoste, A., 2003. A nondestructive tool for the measurement of muscle strength in juvenile oysters *Crassostrea gigas*. Aquaculture 217, 49–60.
Sastry, A.N., 1965. The development and external morphology of pelagic larval and postlarval stages of the bay scallop, *Aequipecten irradians concentricus* say, reared in the laboratory. Bull. Mar. Sci. 15, 417–435.
Squire, J., 2012. The structural basis of muscular contraction[M]. Springer Science & Business Media.
Wanninger, A., 2009. Shaping the things to come: ontogeny of lophotrochozoan neuromuscular systems and the Tetraneuralia concept. Biol. Bull. 216, 293–306.
Wanninger, A., Ruthensteiner, B., Lobenwein, S., Salvenmoser, W., Dictus, J.A.G., Haszprunar, G., 1999. Development of the musculature in the *limpet Patella* (Mollusca, Patellogastropoda). Dev. Genes Evol. 209, 226–238.
Wulf, E., Deboben, A., Bautz, A., Faulstich, H., Wieland, T.H., 1979. Fluorescent phallotoxin, a tool for the visualization of cellular actin. Proc. Natl. Acad. Sci. USA 76, 4498–4502.
Wollesen, T., Wanninger, A., Klussmann-Kolb, A., 2008. Myogenesis in *Aplysia californica* (Cooper, 1863) (Mollusca, Gastropoda, Opisthobranchia) with special focus on muscular remodeling during metamorphosis. J. Morphol. 269, 776–789.
Wurzinger-Mayer, A., Shipway, J.R., Kristof, A., Schwaha, T., Cragg, S.M., Wanninger, A., 2014. Developmental dynamics of myogenesis in the shipworm shipworm *Lyrodus pedicellatus* (Mollusca: Bivalvia). Front. Zool. 11, 90.